Structural health monitoring of a cable-stayed bridge using smart sensor technology: deployment and evaluation

Shinae Jang[1]*, Hongki Jo[1], Soojin Cho[2], Kirill Mechitov[4], Jennifer A. Rice[3],
Sung-Han Sim[1], Hyung-Jo Jung[2], Chung-Bang Yun[2],
Billie F. Spencer, Jr.[1] and Gul Agha[4]

[1]*Department of Civil and Environmental Engineering, University of Illinois, 205 North Mathews Avenue, Urbana, IL 61801, USA*
[2]*Department of Civil and Environmental Engineering, KAIST, 373-1 Guseong-dong, Yuseong-gu, Daejeon 305-701, South Korea*
[3]*Texas Tech University, Lubbock, Texas, USA*
[4]*Department of Computer Science, University of Illinois, 201 North Goodwin Avenue, Urbana, IL 61801, USA*

Abstract. Structural health monitoring (SHM) of civil infrastructure using wireless smart sensor networks (WSSNs) has received significant public attention in recent years. The benefits of WSSNs are that they are low-cost, easy to install, and provide effective data management via on-board computation. This paper reports on the deployment and evaluation of a state-of-the-art WSSN on the new Jindo Bridge, a cable-stayed bridge in South Korea with a 344-m main span and two 70-m side spans. The central components of the WSSN deployment are the Imote2 smart sensor platforms, a custom-designed multimetric sensor boards, base stations, and software provided by the Illinois Structural Health Monitoring Project (ISHMP) Services Toolsuite. In total, 70 sensor nodes and two base stations have been deployed to monitor the bridge using an autonomous SHM application with excessive wind and vibration triggering the system to initiate monitoring. Additionally, the performance of the system is evaluated in terms of hardware durability, software stability, power consumption and energy harvesting capabilities. The Jindo Bridge SHM system constitutes the largest deployment of wireless smart sensors for civil infrastructure monitoring to date. This deployment demonstrates the strong potential of WSSNs for monitoring of large scale civil infrastructure.

1. Introduction

Civil infrastructure systems such as bridges, buildings, pipelines and offshore structures are valuable national assets that must be maintained to ensure economic prosperity and public safety. Many bridge structures in modern countries have reached their design life and will need to be replaced or retrofitted to remain in service. Indeed in the United States, more than 149,000 bridges are structurally deficient or functionally obsolete according to the 2006 report from the Federal Highway Administration (FHWA 2009). Thus, the ability to assess the structural condition and possibly

---

increase the service life has been pursued widely by researchers.

The enabler is structural health monitoring (SHM) – data measurement, system identification and condition assessment. To date, numerous SHM methodologies and systems have been proposed, and some of them have been applied on the full-scale bridge structures: e.g., the Alamosa Canyon Bridge (Doebling *et al.* 1997), the I-10 Bridge (Todd *et al.* 1999), the Hakucho Bridge in Japan (Abe *et al.* 2000), the Bill Emerson Memorial Bridge in Missouri (Çelebi et al. 2004), and the Tsing Ma Bridge in Hong Kong (Wong 2004), to name a few. Though these examples demonstrated the significant potential of SHM, the cost of obtaining the relevant information for SHM on large structures is high (Rice and Spencer 2009). For example, the Bill Emerson Memorial Bridge is instrumented with 84 accelerometer channels with an average cost per channel of over $15 K, including installation.

Wireless smart sensors offer a solution for long-term, scalable SHM of civil infrastructure by providing easier installation and efficient data management at a lower cost than traditional wired monitoring systems. Specifically, the wireless sensor unit used for the monitoring system discussed herein possesses multiple sensor channels and costs less than $500 USD each, including solar power harvesting devices. Moreover, installation time and effort is significantly less than the wired counterpart. Also, wireless smart sensors have on-board computation capability that can help to mitigate the problem of data inundation that is intrinsic to densely instrumented structures. These features of wireless smart sensors help to ensure the scalability of the SHM system to a large network necessary for long-span bridges.

Several researchers have employed wireless smart sensors to monitor bridge structures (Lynch *et al.* 2006, Nagayama and Spencer 2007, Kim *et al.* 2007, Pakzad 2008, Jang *et al.* 2009), providing important insight into the opportunities and challenges for WSSN technology for long-term monitoring. Critical issues identified include: (i) power management, (ii) energy harvesting, (iii) fault tolerance, (iv) autonomous operation, and (v) environmental hardening. To address these research challenges, an international test bed employing a cable-stayed bridge in South Korea was developed.

This paper reports on the deployment and evaluation of a state-of-the-art WSSN on the Jindo Bridge. This effort is part of a trilateral collaboration between the USA (University of Illinois at Urbana-Champaign), South Korea (Korean Advanced Institute of Science and Technology, KAIST) and Japan (University of Tokyo). The test bed bridge has a 344-m main span and two 70-m side spans, connecting mainland South Korea with Jindo Island across the sea. The main components of the WSSN deployment are the Imote2s (Crossbow Technology 2009), custom-designed multimetric sensor boards, base stations, and software provided by the ISHMP Services Toolsuite (Rice and Spencer 2009). Although the functionality and the stability of each component has been previously verified by a series of experiments both at the laboratory scale and for small full-scale bridges, various factors at the monitoring site make this deployment quite challenging and will be discussed in this paper. In total, 70 sensor nodes and two base stations have been deployed to monitor the bridge using an autonomous SHM application with excessive wind and vibration triggering the system to initiate monitoring. Finally, the performance of the system has been evaluated in terms of hardware durability, software stability, power consumption and energy harvesting options.

2. Bridge description

The Jindo Bridges are twin cable-stayed bridges connecting Haenam on the mainland with the

Fig. 1 1st (right) and 2nd (left) Jindo Bridges

Jindo Island (see Fig. 1). The Jindo Island is the third largest island in South Korea, and Haenam, which is located in the south-west tip of the Korean peninsula. Each of these bridges consists of three continuous spans, with a 344-m central main span and two 70-m side spans.

The original Jindo Bridge, constructed in 1984 by Hyundai Engineering & Construction Co., Ltd., was the first cable-stayed bridge in South Korea. The width of the bridge is 11.7-m, the design traffic velocity is 60 km/hr, and the design live load is based on AASHTO HS-20-44 (DB-18). The second Jindo Bridge was constructed in 2006 by Hyundai Engineering & Construction Co., Ltd., Daelim Industrial Co., Ltd. and Namhei Co., Ltd. The width of the second bridge is 12.55 m, the

(a) Elevation

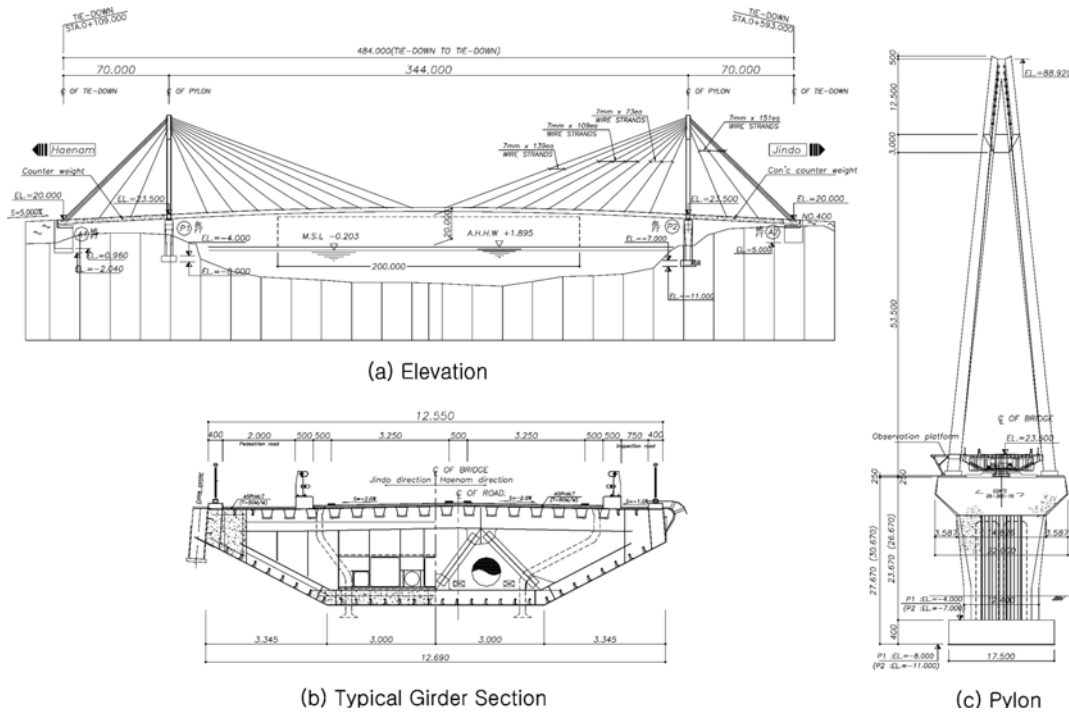(b) Typical Girder Section

(c) Pylon

Fig. 2 Bridge drawings (2nd Jindo Bridge)

traffic design velocity is 70 km/hr, and the design live load is based on AASHTO HS-20-44 (DB-24, DL-24). It has a streamlined steel box girder supported by 60 high-strength steel cables connected to two pylons. The structural drawing of the bridge is shown in Fig. 2.

   Both bridges have existing SHM systems based on wired sensors. The first Jindo Bridge has 38 strain gages, four inclinometers, two anemometers, two seismic accelerometers, five uniaxial capacitive accelerometers, and 15 uniaxial piezoelectric accelerometers. The second Jindo Bridge has 15 thermometers, 15 strain gages, four biaxial inclinometers, two string pots, two laser displacement meters, 24 Fiber Bragg Grating sensors, 20 uniaxial capacitive accelerometers, two biaxial force balance type accelerometers, and three triaxial seismic accelerometers. Among two bridges, the second Jindo Bridge is selected as the test bed for this research, for two primary reasons: (i) the existing SHM system is quite versatile, including accelerometers and fiber optic sensors and (ii) the design and construction documents are more complete.

3. Bridge monitoring system

3.1 Hardware

   The wireless smart sensor is the key element of the bridge monitoring system. Two hardware configurations are employed: a gateway node attached to the base station PC, and battery-operated leaf nodes at remote locations to the base station. Because the wind excitation is the major source of bridge vibration, two types of sensor boards have been employed: the SHM-A sensor board to measure vibrations and the SHM-W sensor board to measure signals from an anemometer. To evaluate the potential for long-term deployment, solar panels and rechargeable batteries have been installed on selected nodes.

3.1.1 Smart sensor nodes

   Each smart sensor unit consists of an Imote2, an IBB2400CA battery board, and the SHM-A multi-scale sensor board. The Imote2 is a high-performance wireless smart sensor platform, having Intel's PXA271 XScale® processor running at 13-416 MHz and an MMX DSP Coprocessor (Crossbow Technology 2007). The memory size is increased significantly from the previous generation of motes, having 256 kB SRAM, 32 MB FLASH and 32 MB SDRAM, which enables longer measurements, as well as the on-board computation. The IBB2400CA battery board is designed to power the Imote2 using three 1.5-volt batteries.

   The SHM-A sensor board has been designed for monitoring civil infrastructure through the Illinois SHM Project, an interdisciplinary collaborative effort by researchers in civil engineering and computer science at the University of Illinois at Urbana-Champaign (Rice *et al*. 2010). The tri-axial accelerometer employed is the ST Microelectronic's LIS344ALH, which has a range of ±2 g. The analog acceleration signals from the accelerometers are digitized by the Quickfilter QF4A512, which has a 4-channel, 16-bit Analog to Digital Converter (ADC) and programmable signal conditioner with user-selectable sampling rates and programmable digital filters. The resolution of the ADC is 16 bit, and the noise levels of the accelerometer are 0.3 mg for the x- and y-axes and 0.7 mg for the z-axis. The SHM-A board also contains temperature, humidity and light sensors. An additional analog input allows this board to measure data from many other types of sensors such as anemometers and strain gages. Four sampling frequencies (10, 25, 50, 100 Hz) have been pre-programmed on the
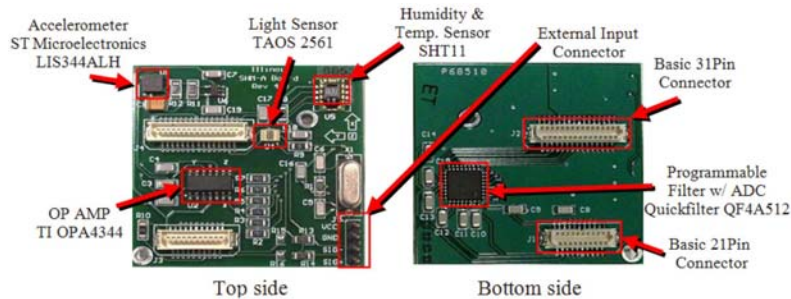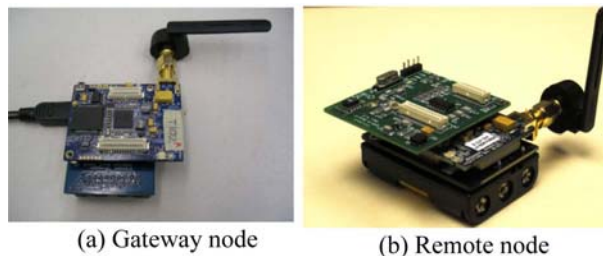
Fig. 3 SHM-A sensor board (Rice *et al.* 2010)

(a) Gateway node   (b) Remote node

Fig. 4 Smart sensor units

SHM-A board for this bridge monitoring application; however, the sampling rate can be chosen nearly arbitrarily by designing appropriate filters for the QF4A512. The components of the SHM-A sensor board are identified in Fig. 3. More details can be found in (Rice *et al*. 2010).

Two hardware configurations of smart sensor nodes are required for the wireless communication and sensing: a gateway node for sending commands and receiving wireless data from the network, and the battery-powered nodes remote to the base station. The gateway node consists of an Imote2 stacked on an IIB2400 interface board connected to the base station PC via a USB/UART port. The leaf nodes consist of an SHM-A sensor board and Imote2 stacked on the battery board as shown in Fig. 4. To increase the communication range, both nodes are equipped with an Antenova gigaNova Titanis 2.4 GHz external antenna (Antenova 2009). The sensor nodes are placed in environmentally hardened enclosures to endure the harsh environment at the Jindo Bridge site.

3.1.2 Wind monitoring system: modified SHM-A board with anemometer

The Jindo Island is located in Haenam, one of the windiest regions in South Korea with several typhoons each year. A cable-stayed bridge like the Jindo Bridge is sensitive to such strong wind; thus, an important objective of this study is monitoring the wind and the associated dynamic responses of the bridge.

A 3-D ultra-sonic anemometer has been incorporated into the WSSN for reliable wind monitoring of the Jindo Bridge. Because of its high resolution (wind speed: 0.01 m/s, wind direction: 0.1 degree) and good accuracy (wind speed: ±1%, wind direction: ±2 degrees), the RM Young Model 81000 anemometer was chosen (see Fig. 5(a)). The durability of ultra-sonic anemometers makes them well-suited for long-term operation in harsh environment. Moreover, the anemometer's analog voltage outputs, ranging from 0 to 5V, can be easily accommodated by the SHM-A board with

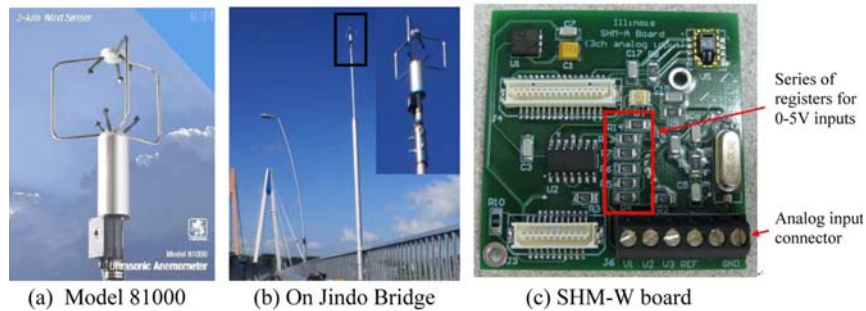(a) Model 81000	(b) On Jindo Bridge	(c) SHM-W board

Fig. 5 3D ultra-sonic anemometer (Model 81000, RM Young) and SHM-W board

small modifications.

The SHM-W board is developed by modifying the SHM-A board to have three external 0-5V input channels and one acceleration channel. The wind speed (channel 1), horizontal and vertical wind directions (channels 2 and 3) are measured through analog input interface connectors on the SHM-W board as shown in Fig. 5(c). Because the SHM-W board also uses the QFA512-based sensor board, it uses the same software drivers as the SHM-A board; as a result, the wind data is acquired precisely synchronized with the acceleration data from the SHM-A board. Another modification for SHM-W board is that it is adjusted so to that the full range of the 0-5V inputs is utilized, resulting in better resolutions for the wind data.

3.1.3 Energy harvesting with solar panels

While battery power provides a convenient and readily-available solution for WSSNs, the drawback is that regular battery replacements are required for long-term deployments. From this perspective, energy harvesting is important for long-term operation of the wireless SHM systems. Roundy *et al.* (2004) compared the power densities of available harvesting sources such as sunlight, thermal gradient, human motion, vibration and acoustic noise, etc. As shown in Table 1, the power density of the solar cells is the largest, showing the potential to increase the network lifetime to longer than one year. Therefore, solar panels and rechargeable batteries have been chosen as energy the harvesting/power system and installed on several leaf nodes at locations where battery replacement is difficult.

The Imote2 can be powered by rechargeable batteries using the Power Management Integrated Circuit (PMIC) (Miller and Spencer 2009). The PMIC can be connected directly to Lithium-Ion or Lithium-Polymer batteries without a protection diode; the diode can be bypassed with an additional zero-ohm resistor (R1). To allow the current from solar panel to flow into the battery, the nCHARGE-EN pin, which is a control switch to decide battery options, should be pulled low with

Table 1 Power densities of harvesting technologies (Roundy *et al.* 2004)

Harvesting technology	Power density
Solar cells (outdoors at noon)	15 mW/cm^2
Piezoelectric (shoe inserts)	330 μW/cm^3
Vibration (small microwave oven)	116 μW/cm^3
Thermoelectric (10 $^{\circ}$C gradient)	40 μW/cm^3
Acoustic noise (100 dB)	960 nW/cm^3

(a) Power supply options for Imote2 (Crossbow Technology 2007)   (b) Battery board modifications
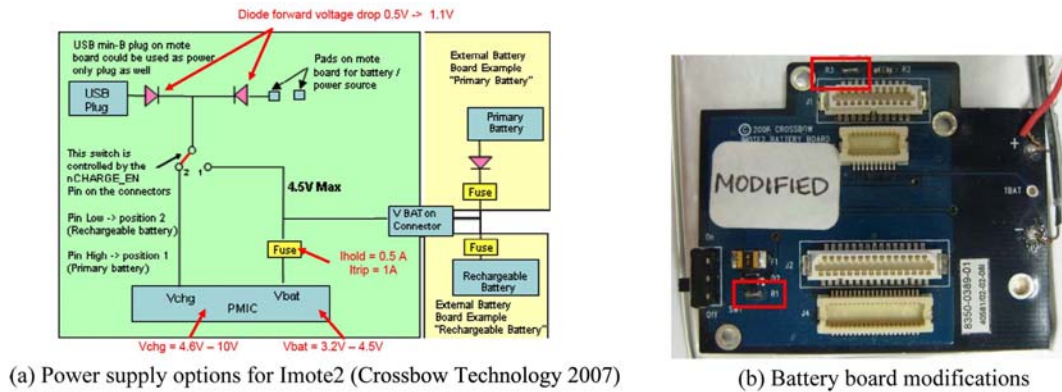
Fig. 6 Power supply options for Imote2 and battery board modification for recharging option

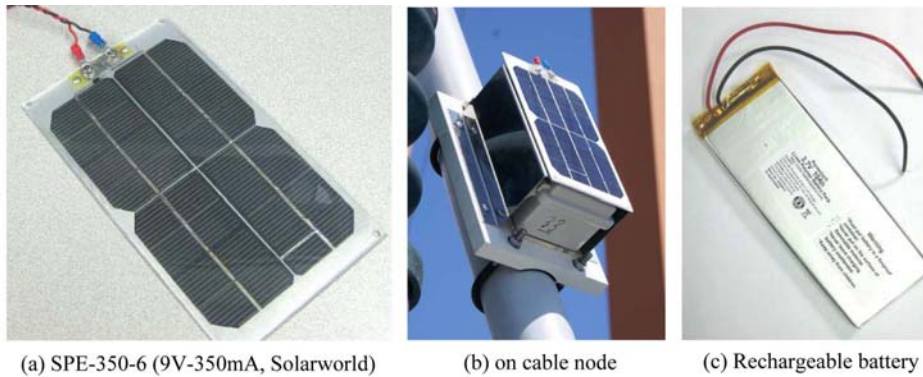(a) SPE-350-6 (9V-350mA, Solarworld)   (b) on cable node   (c) Rechargeable battery

Fig. 7 Solar panel and rechargeable battery for Jindo Bridge SHM

the another zero-ohm resistor (R3) on the battery board (see Fig. 6).

Considering the range of input power that the Imote2 can support (4.6~10 V, up to 1400 mA), the SPE-350-6 solar panel from Solarworld (9 V-350 mA) shown in Fig. 7(a) was employed. A Powerizer lithium-polymer rechargeable battery (Powerizer 2009) was selected, which reaches up to 4.2 V when fully charged. This system has 10,000 mAh capacity (half of that of D-cell batteries), will allows this system to supply power to the Imote2 for an extended period without recharging.

3.2 Software: ISHMP services toolsuite

The Illinois SHM Project developed a suite of services, denoted the ISHMP Services Toolsuite, that implements key middleware functionality to provide high-quality sensor data and to transfer the data reliably to the base station via wireless communication across the sensor network, and a library of numerical algorithms. This open-source software is available at http://shm.cs.uiuc.edu/software.html. More detailed information regarding this software can be found in Rice *et al*. (2010).

The toolsuite components are categorized into foundation services, application services, tools and utilities, and continuous and autonomous monitoring services. The foundation services provide the fundamental functionalities to measure synchronized sensor data reliably (Mechitov *et al.* 2004,

Nagayama and Spencer 2007, Rice *et al.* 2008). The application services are the numerical algorithms to implement SHM applications on the Imote2, including modal identification and damage detection algorithms. The tools and utilities support network maintenance and debugging. This category has essential services for full-scale monitoring as well as sensor maintenance. The key features of these services include *RemoteSensing,* a remote data measurement application; *DecentralizedData Aggretation,* data measurement and on-board computation to calculate the correlation functions for decentralized local groups; *imote2comm* and *autocomm,* an automatic terminal tool to interact between the base station PC and a gateway node; *Vbat*, a command for checking a leaf node's battery level; *TestRadio,* a tool for assessing radio communication quality, and many others.

The continuous and autonomous monitoring service critical for this deployment is *AutoMonitor*, an autonomous SHM network management application, which combines *RemoteSensing*, *ThresholdSentry*, and *SnoozeAlarm* (Rice and Spencer 2009). *SnoozeAlarm* is a strategy that allows the network to sleep most of the time, thus improving energy efficiency and allowing long-term system deployment. To wake the network for an important event, the *ThresholdSentry* application defines a specified number of the leaf nodes as sentry nodes. The sentry nodes wake up at predefined times and measure a short period of acceleration or wind data. When the measured data exceeds a pre-defined threshold, the sentry node sends an alarm to the gateway node, which subsequently wakes the entire network for synchronized data measurement. In this way, *AutoMonitor* enables the automatic, continuous monitoring with reduced power consumption.

The *AutoMonitor* application employs multiple threshold levels for the Jindo Bridge SHM system. When a single threshold level is used to define the maximum number of events during given period, if the threshold level is too high, the data measurements would rarely if ever occur. If too small a threshold level is used, the number of events can be exhausted with small structural responses, hence possible strong vibrations during remaining period cannot be captured. The multiple threshold levels, having separate maximum number of events, make it possible to measure both rare but strong responses and frequent but low-level ambient vibration during a given period, which enables more effective SHM.

Another feature of the *AutoMonitor* application is a wind threshold sentry. The wind sentry node is equipped with SHM-W sensor board with ultrasonic anemometer. Strong winds, such as those that occur during typhoons, induce large structural responses. Therefore, the wind sentry will trigger network sensing when the velocity exceeds a threshold. In this deployment, both vibration- and wind-based sentry nodes have been installed for the *AutoMonitor* application. In summary, the final software version is the *AutoMonitor* application having both data measurement and on-board computational functionality, a multiple threshold triggering strategy using vibration/wind sentries pursuing energy efficiency using *SnoozeAlarm.*

4. Deployment of the SHM system

The developed hardware and software framework has been deployed on the Jindo Bridge to realize the first large-scale, autonomous, WSSN-based SHM system. Due to the harsh environment at the site, the delicate electrical components of the SHM system have been hardened to prevent corrosion, overheating, or other damage. Also, many verification and optimization steps have been required to extend the laboratory-scale SHM system to a full-scale deployment for a long-span bridge structure. The details of the hardening and optimization process are provided in this section.

4.1 Network topology

The network topology is carefully determined to ensure reliable network sensing for the Jindo Bridge. The major factors to define the network topology are the size of network, the communication range, etc. The total length of the bridge is 484 m, the communication range of Imote2 with external antenna is ~200 m, and the number of sensor nodes in network is 70. Considering the range and the communication time, the network was divided into two sub-networks: one on the Jindo side and the other on the Haenam side.

The Jindo sub-network consists of 33 nodes with 22 nodes on the deck, three nodes on the pylon, and eight nodes on the cables. The Haenam sub-network consists of 37 nodes with 26 nodes on the deck, three nodes on the pylon, and seven nodes on the cables. Each sub-network is controlled by a base station located on the concrete piers supporting the steel pylons of the first Jindo Bridge. These locations were chosen to achieve consistent line-of-site communication with leaf nodes.

4.2 Base station

4.2.1 Components of base station

Because the base station provides access to the WSSN, it is critical to the performance of the entire network. The base station controls the network by 1) sending messages to the leaf nodes, 2) storing the transmitted data from the WSSN, 3) processing received data and 4) transferring the data to the remote server via internet. To achieve these functions, the base station is composed of an industrial-grade PC running Windows XP Professional OS, an uninterrupted power supply (UPS) backup, a gateway node and an environmentally hardened enclosure as shown in Fig. 8.
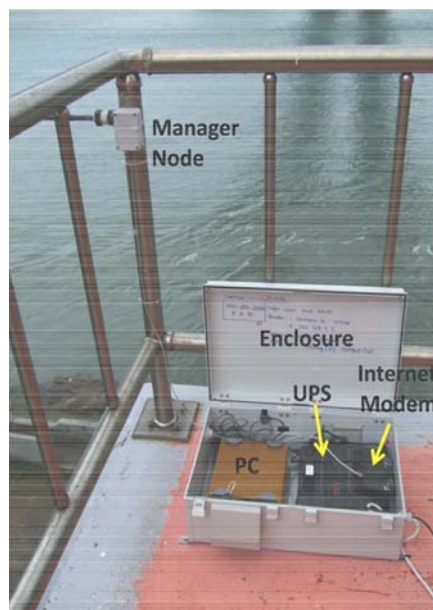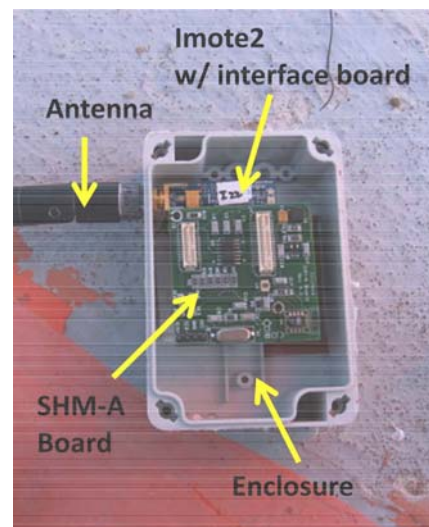

Fig. 8 Base station

Fig. 9 Gateway node

An industrial-grade PC AAEON AEC-6905 was adopted as a base station for its fan-less architecture, protecting it from dust and moisture. The UPS backup APC ES550 protects the base station components from an unexpected electric surges and outages. The gateway node is consisted of an Imote2 stacked with an interface board for interactive serial communication and SHM-A sensor board and 2.4 GHz 5 dBi dipole antenna as shown in Fig. 9. A wired internet line was installed to the PC with an ADSL internet modem to provide remote access to base station, to control the WSSN, and to download the measured data.

Software for remote control and data download is installed on the base station. On the top of basic OS and anti-virus software, the key components of software are Cygwin and the *autocomm* executable application for interfacing with the gateway node, the VNC (Virtual Network Computing) server for remote desktop control, and an FTP (File Transfer Protocol) server to remotely download the measured data.

4.2.2 Environmental concerns and solutions

The environmental solution for stability of the base stations is provided when it is exposed to environmental load such as sunlight, rain, snow, fog and typhoon. The site of the Jindo Bridge is often subject to high humidity due to frequent fog and harsh winds. To protect electric components from damage, ABS enclosures were employed to house the base stations. This industrial-grade PC was found to radiate significant heat, which results in shut down of the PC by drastically increasing the temperature inside the enclosure. To address this problem, the enclosure was modified to include two-way ventilation as shown in Fig. 10. All ventilation openings have anti-bug nets and rain-protection brackets, and the exhaust fan is connected to a temperature sensor inside the enclosure. If the temperature in the enclosure is over 35 ℃, the fan will automatically turn on. In addition, the power cable, the USB cable to the gateway node, and the LAN cable to the wired internet line pass through the enclosure wall via cable glands. This enclosure with the ventilation system has provided effective and stable operation of the base station.
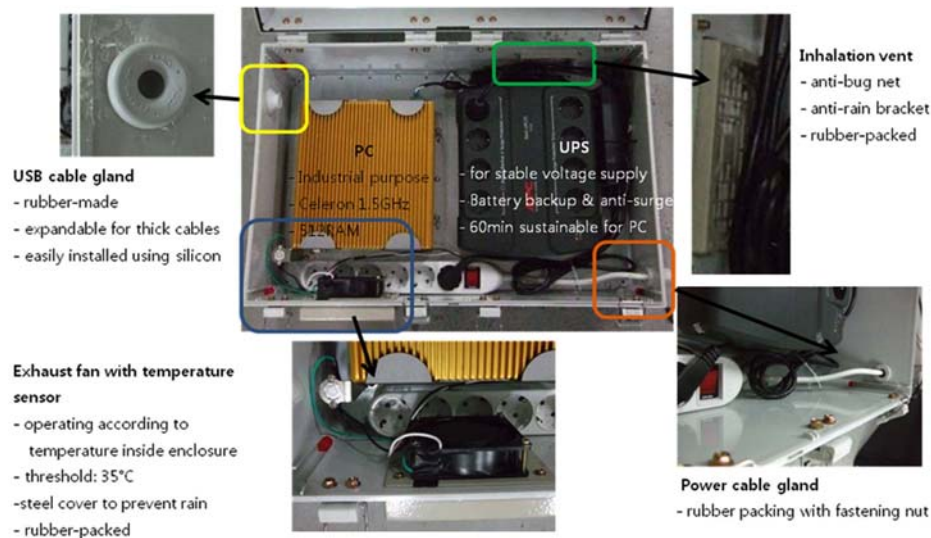

Fig. 10 Ventilation enhancements for base station enclosure

4.3 Smart sensor nodes

4.3.1 Environmental hardening and sensor installation

The leaf nodes were also placed in environmentally hardened enclosures. Water-tight PVC enclosures were employed protecting from moisture as well as not interfering with radio communication as shown in Fig. 11. The battery board is modified to employ three D-cell batteries instead of standard AAA batteries. The nominal voltage of both a single AAA and a single D-cell battery is 1.5V, while the capacity of an alkaline D-cell battery is 20,000 mAh, versus 1,200 mAh for an AAA alkaline battery; thus, enabling significantly longer network operation. The size of the enclosure is primarily dependent on the size of the batteries.

To increase the radio communication range, the Imote2 has been modified to use an external antenna (Linderman *et al.* 2010: Antenova gigaNova Titanis 2.4 GHz external antenna (Antenova 2009). The external antenna is mounted to the enclosure and then connected to the Imote2 with an antenna extension cable. The sensor unit is mounted separately from the battery holder. The bottom of the battery board is attached on the enclosure using the Scotch® Exterior Mounting Tape.

The smart sensor nodes for the deck, pylons and cables are mounted using different methods. The leaf nodes on the deck are mounted upside down on the bottom side of deck using magnets. The leaf nodes on the pylons also employed the magnets for attachment. This magnet is one-directional and has 10 kg holding capacity (Fig. 12(a)). Using two magnets on the bottom of each enclosure, the secure connection between the sensor enclosure and the bridge steel surface is ensured. In addition, the magnets are surrounded by double-sticky Styrofoam panel with the thickness of the
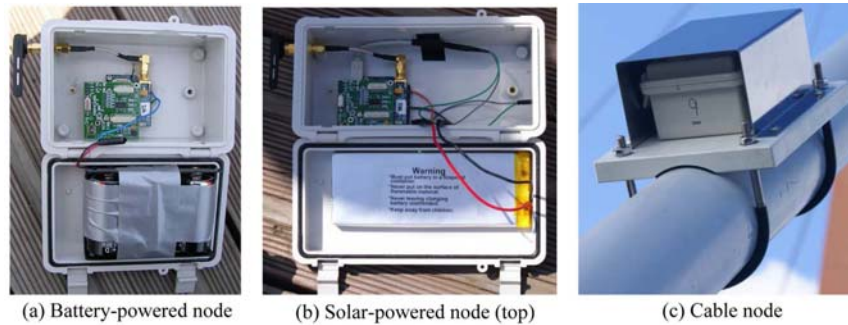

(a) Battery-powered node   (b) Solar-powered node (top)   (c) Cable node

Fig. 11 Hardened sensor nodes

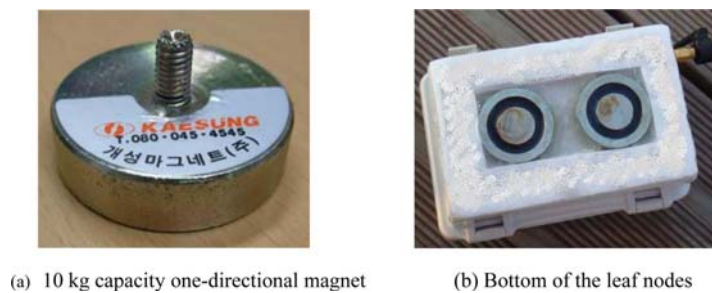(a) 10 kg capacity one-directional magnet   (b) Bottom of the leaf nodes

Fig. 12 Magnet-based sensor attachment

magnet, to prevent the vibration due to the vortex-shedding in the gap between the enclosure and structure surface (see Fig. 12(b)). This approach reduces the installation time and effort under the deck; however, the magnet-based method is not feasible for the cable sensors due to round surface. Therefore, the leaf nodes on the cables are mounted using two U-bars and aluminum mounting plate as shown in Fig. 11(c). Because these nodes are directly exposed to sun light, the stainless steel cover is employed to protect the PVC enclosure.

4.3.2 Software setup and verification

Two software configurations have employed to prepare the smart sensor nodes. The gateway nodes have been programmed with the *AutoMonitor* application to control the autonomous monitoring of the network. The leaf nodes have been programmed with the *RemoteSensing*, which combined with *TestRadio,* and *DecentralizedDataAggregation* (Sim and Spencer 2009). In the *AutoMonitor* application, users can decide whether raw acceleration data or correlation functions using decentralized estimation from the local groups are returned to the base station by selecting either *RemoteSensing* or *DecentralizedDataAggregation*, respectively.

The software performance using a large network of wireless smart sensor nodes have been previously verified both in the laboratory and field environments after programming the nodes. After loading the software, a number of autonomous monitoring application tests were conducted to check the performance both in the laboratory and the field. The purpose of these tests is to verify the long-term network stability under various operation scenarios with 40 nodes. During the tests, basic communication parameters were modified to accommodate the large network size.

Fault tolerance features for robustness of the software have also developed because a human operator cannot constantly monitor the state of the monitoring system. To this end, the *AutoMonitor* application provides several features, including: (1) sending the network wake-up command repeatedly, as in some cases a node can return to the sleep mode soon after waking up, (2) skipping over unresponsive nodes after a short timeout when sending commands or receiving data, and (3) rebooting the leaf nodes in case of failures of component services that may leave the node in an inconsistent state and prevent further operation. Additionally, the *AutoMonitor* application coordinates with its component services (*SnoozeAlarm*, *ThresholdSentry* and *RemoteSensing*) to handle internal errors in those services in a consistent manner. After the software setup and verification was completed, all leaf nodes were deployed on the bridge at the locations indicated in Fig. 14.

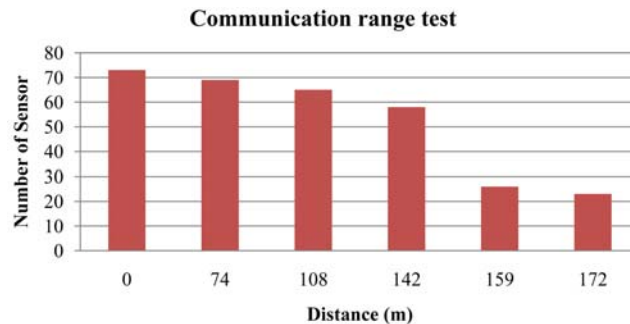### 4.3.3 Communication range tests for sensor placement

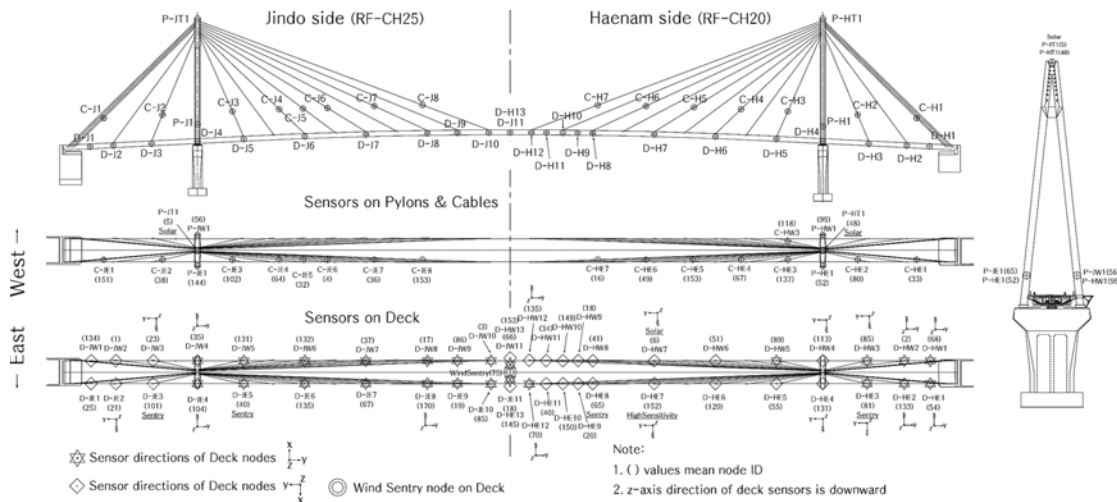Fig. 13 Communication range test (73 sensors tested)

Fig. 14 Sensor locations

Because single-hop communication was used for this deployment, radio communication tests were conducted on-sight using the *TestRadio* application to measure the packet reception rates at various communication distances. During the communication range tests, the gateway node was located at the Haenam side pylon and the leaf nodes were gradually moved out to the mid-span. The number of sensors which were unresponsive to the *TestRadio* request from the gateway node was counted as shown in Fig. 13. In total, 73 Imote2s were tested and five nodes were found to be unresponsive and subsequently replaced. At the mid-span at 172 m, 23 Imote2s were found to communicate effectively. Based on these radio communication tests, sensors location were optimized as shown in Fig. 14.

4.3.4 Optimal antenna direction

The antenna orientation is optimized based on the influences of network environment to determine optimal network performance. The antennas should be co-linear, to ensure optimal radio communication. The electric field component in the desired orientation is referred to as the co-polarized field and any field in the perpendicular (undesired) direction is referred to as the cross-polarized field (Linderman *et al*. 2010). Optimizing the antenna orientation is not a simple problem for large WSSNs because elevations of sensors are different for those under the deck, at the side of the pylon, on the top of the pylon and the cable nodes. The antenna direction of the gateway node is critical to reliable communication with all leaf nodes. Therefore, the antenna for the gateway node and all leaf nodes are oriented perpendicular to the longitudinal axis of the bridge and parallel to the ground as shown in Fig. 15. In this manner, all sensors can communicate with the gateway node efficiently. This configuration has been verified through communication tests.

5. Communication parameter optimization

The communication parameters have been optimized to operate the large WSSN on a long-span
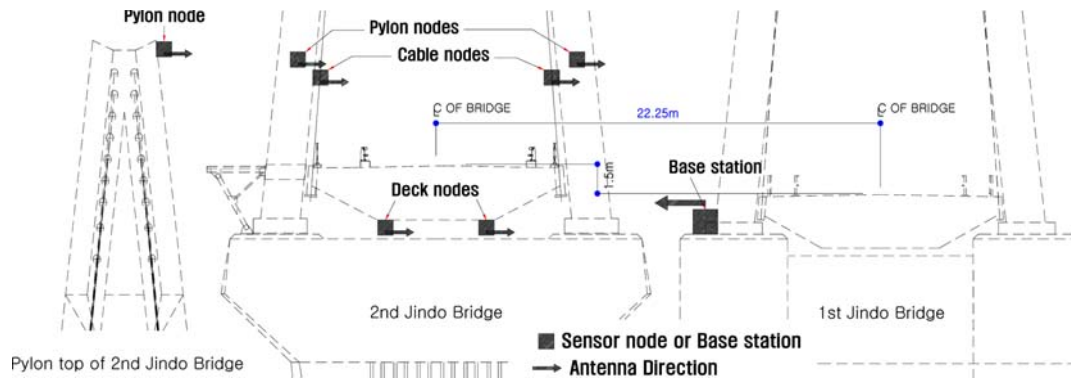
Fig. 15 Antenna orientation

Table 2 Software parameters for the Jindo Bridge deployment

Category	Parameter	Initial state	Updated state
RemoteSensing	Number of *RemoteSensing* events	1 per day	4 per day
	Time synchronization wait time	30 sec	30 sec
	SENSING START DELAY	15,000	50,000
	NODE SENSING START DELAY	1,000	1,500
	Sampling frequency	50 Hz	10 Hz
	Channels sampled	3	3
	Number of data points	1,000	5,000
Snooze Alarm	*SnoozeAlarm* wake/listen time	750 ms	750 ms
	SnoozeAlarm sleep time	15 sec	15 sec
	SnoozeAlarm duty cycle	4.76%	4.76%
ThresholdSentry	*ThresholdSentry* check interval	20 min	10 min
	ThresholdSentry sensing time	10 sec	10 sec
	Threshold value for vibration sentry	10 mg	10 mg, 50 mg
	Threshold value for wind sentry	N/A	3 m/sec, 8 m/sec
Watchdog Timer	Period	10 min	60 min
	Update	1 min	60 min

bridge in terms of *RemoteSensing*, *DecentralizeDataAggregation*, *SnoozeAlarm*, *ThresholdSentry* and *Watchdog Timer*. Table 2 shows the list of the network parameters and values for the initial state and the updated state. First of all, the number of times that the *RemoteSensing* application can be run is updated from once per day to four times a day. The primary concern for the number of measurement events is the power consumption. After pre-deployment with the initial parameters, it was found that the maximum number of the measurement events could be increased to four times a day without significantly increasing the power consumption of the WSSN.

The communication waiting times are important for successful operation of *RemoteSensing* with large networks of smart sensors. There are four steps in *RemoteSensing*: (1) network time synchronization, (2) sending measurement parameters from the gateway to leaf nodes, (3) data collection and (4) transferring data back to the gateway node and saving the data on the base station. The first communication wait time is for time synchronization. The second wait time is the time required to

send the sensing parameters to all of the nodes in the network. This total wait time is expressed by

$$T = S_c + n \cdot S_n \qquad (1)$$

where, S_c is a constant wait time, S_n is a short nodal wait time for each sensor denoted as, and n is the number of sensors. These two parameters are increased in the updated state considerably because the communication took a longer time for the long distances between the leaf nodes.

The data measurement parameters include the sampling frequency, the measurement directions, and the number of data point for each channel. 10,000 data points are measured in three directions at 10 Hz.

The *SnoozeAlarm* parameters include the duration of the wake/listen time and the sleep time. The sleep time can be chosen based on the target excitation. For Jindo Bridge, loading from strong winds from typhoons having a duration of several hours to a day is significant. For such excitations, waking the network up within several minutes of a trigger event is quite reasonable. To accommodate this, the deep sleep interval is set to 15 seconds, and the wakeup time to listen for commands is 750 ms. With this setup, the wake up time for the entire network was in the range of 1~5 minutes based on the radio communication conditions.

The *ThresholdSentry* parameters include the number of sentry nodes used in the network. The number of sentry nodes for this deployment is three for Haenam side and two for Jindo side. The sentry checks the acceleration level frequently to catch large vibration due to strong winds. The sentries are set to wake up every 10 minutes and measure the acceleration for 10 seconds. The threshold values for the vibration sentry are 10 mg and 50 mg, so that large vibration events more than 50 mg should be recorded. For the wind sentry, the thresholds are 3 m/sec and 8 m/sec to measure both the usual state of wind-induced vibration (3-4 m/sec) and stronger wind vibration events.

Finally, a *Watchdog Timer* is used to reset the nodes to ensure the network reliability in the case of a node hanging due to some unexpected error. The *Watchdog* update time is the waiting time before the processor resets the node when the node gets hung. Using this setup, an indefinite hang-up of nodes may be avoided. The *Watchdog* period should be longer than the measurement duration so that the *Watchdog* timer does not interrupt the measurement and reset the leaf nodes. The *Watchdog* update was set to one minute, and the *Watchdog* timer period is set to 10 minutes during the initial state, because the network sensing takes less than 10 minutes. This is updated to 60 minutes and 60 minutes respectively for the updated state to measure longer data with increased distances of sensor distribution.

6. Evaluation of the SHM system

6.1 Hardware performance

The hardware components including smart sensor nodes base stations and the anemometer with many installation details have shown reliable performance during this deployment. One of the biggest enablers of the deployment on the Jindo Bridge is the SHM-A sensor board. The resolution of the sensor board is ~0.3 mg and adequate to measure the bridge vibration in the range of 5~30 mg. The programmable sampling frequency features are critical to capture major natural frequencies of the bridge under 1 Hz as opposed to ITS400CA basic sensor board (MEMSIC 2010) support higher sampling frequency than 280 Hz. Furthermore, the modified SHM-A board with an anemometer, the

SHM-W sensor board, has reliably measured the wind information; however, the horizontal component of the wind direction is not measured by channel 2 of the SHM-W board because of a hardware malfunctioning problem on the anemometer.

The two base stations have been functioning reliably for four months, enabling stable remote monitoring of the Jindo Bridge and communication with each gateway node. When checking the condition of the inside of the base station enclosure after four months of operation, it was confirmed that it has successfully protected the computer from overheating and the harsh environment.

The enclosures for the leaf nodes have also performed well. The inside of sensor enclosure was dry and the temperature was acceptable. The magnet-based attachment has proven to be an excellent solution for the Jindo Bridge because all leaf nodes have been attached firmly for four months.

6.2 Software performance

The *AutoMonitor* application has shown stable performance after appropriate optimization of the sensing and radio communication parameters. All software is operating reliably and remotely desktop using a VNC® server. *RemoteSensing* and *DecentralizedDataAggregation* work successfully with optimized communication parameters.

The ambient vibration data at the Jindo Bridge has been acquired from the WSSN. One sample of recorded data has shown in Fig. 16, of which levels are ~8 mg, ~40 mg, ~5 mg for the deck, cable and pylon, respectively.

The power spectral densities (PSD) of the vibration data have been investigated. Fig. 17(a) shows the PSDs of the deck vibrations at the mid span, quarter span and at the pylon. The PSD magnitude of deck sensors near pylon is almost zero; however, the other two sensors at the mid span and the quarter span show significant energy around 0.44, 0.66 and 1.03 Hz, implying the natural frequencies of the bridge. Fig. 17(b) shows the comparison between the PSD from the existing wired sensor at the quarter span and the PSD from the deployed wireless sensor at the same location. Though the wired sensor data was measured in 2007 and the wireless sensor data was measured in 2009, most natural frequencies agree well with the previous data.

Fig. 18 shows the PSD from six cables sensors and from the pylon sensors the one in the side and at the top. For the cable sensors, the consistent peaks are shown around 0.44, 0.66, 1.03 Hz for all sensors and different peaks for various cables in other frequency regions. The natural
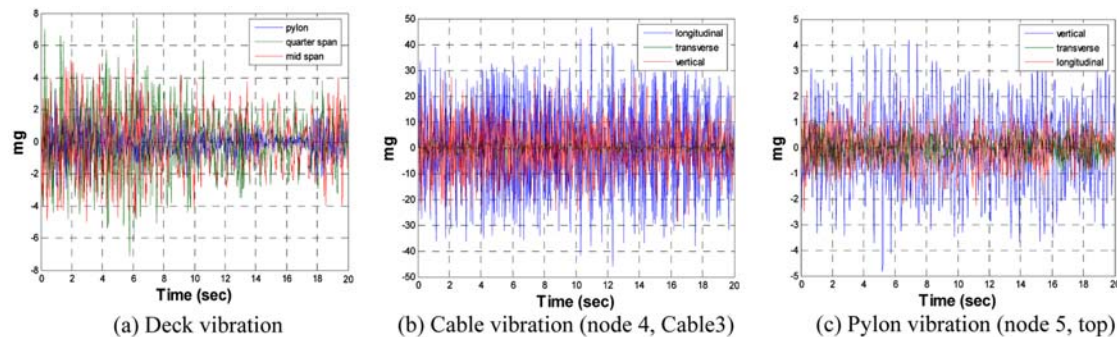

(a) Deck vibration   (b) Cable vibration (node 4, Cable3)   (c) Pylon vibration (node 5, top)

Fig. 16 Acceleration on the Jindo side on 6/12/2009 at 04:50PM

(a) Deck vibration (7/18/2009)

(b) Comparison with wired data measured in 2007
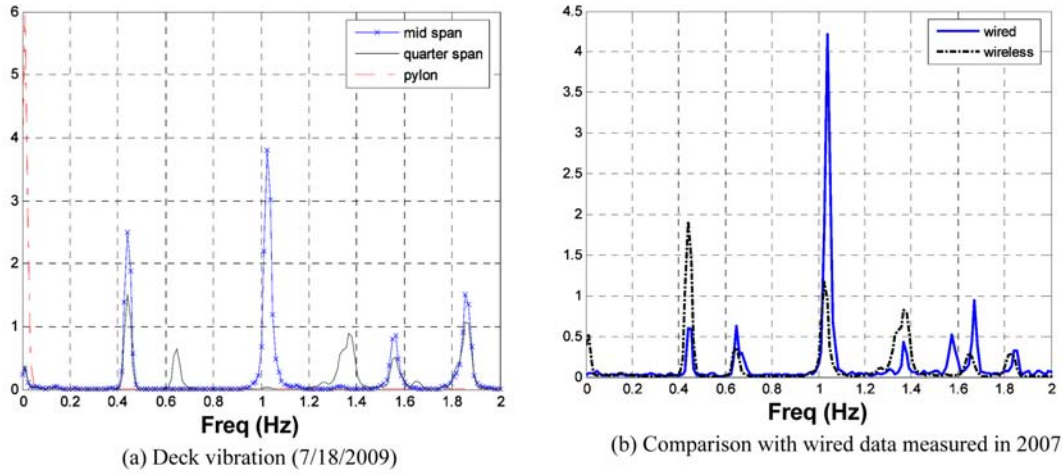
Fig. 17 Power spectral density comparison at the quarter span of the Jindo Side

(a) Cable vibration of 6 sensors

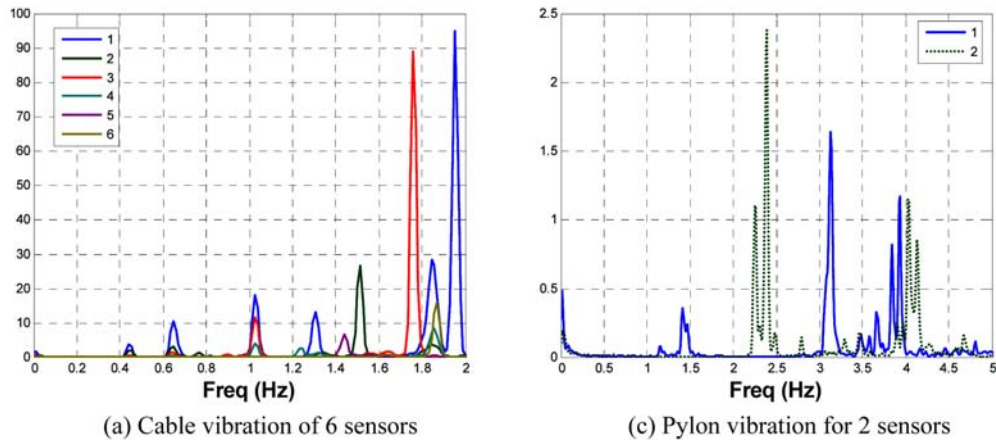(c) Pylon vibration for 2 sensors

Fig. 18 Power spectral densities on 7/18/2009

frequencies of the pylon sensor in the side (1) and of the one at the top are different. Detailed modal analysis and detailed cable tension estimation is described in the companion paper in this issue (Cho *et al*. 2010).

6.3 Wind speed and direction

The wind speed and direction has been successfully measured using the 3D ultra-sonic anemometer at the mid span. The outputs of the SHM-W sensor board are raw voltage measurements from the anemometer. This data have been converted to the wind speed and voltage using the anemometer sensitivity. The data are synchronized with vibration data measured by SHM-A sensor board. Fig. 19 shows example data. In this sample data, the wind speed was 4-6 m/sec and the direction is zero degrees to the longitudinal direction of the bridge.
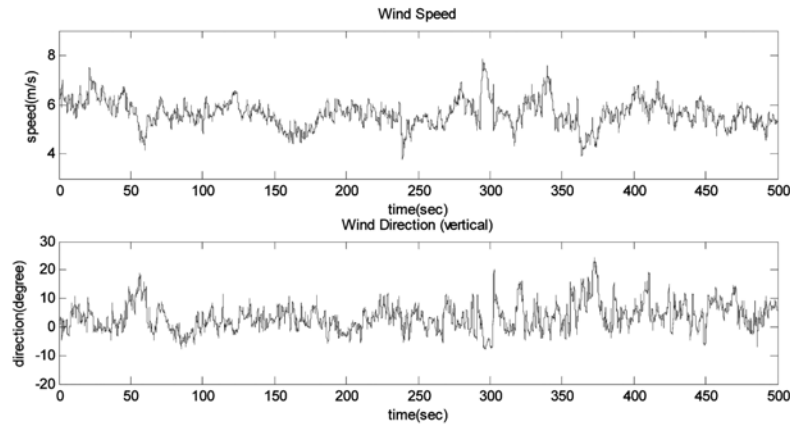
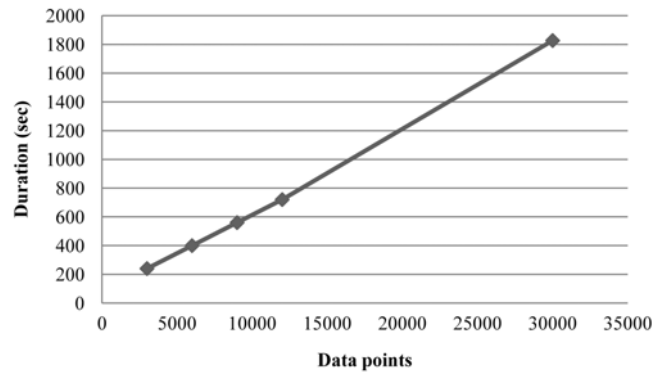Fig. 19 Wind data measured at 06:33 AM on 9/8/2009

Fig. 20 Communication time of 23 sensor nodes based on the number of data points collected

Fig. 20 shows the operating time for the *RemoteSensing* application in terms of various phases for different requested sample sizes. In total, three axes of accelerations were measured at 50 Hz from 23 sensor nodes. In this specific deployment, the communication time sending data back to the gateway node has been measured. Although the total communication time depends on various environmental and communication factors, the communication time shows a linear relationship with the number of requested data points as shown in Fig. 20. Based on this result, the total communication time to acquire 30,000 points from 46 sensor nodes of two networks is about 30 minutes.

6.4 Power consumption

The battery voltage levels for all nodes in both sides have been recorded for two months as shown in Fig. 21. The average initial voltage of the three D-cell batteries on each sensor nodes was 4.6 V, and the average on board voltage reading using *RemoteVbat* command was 4.2 V. The on board voltage reading is 0.3~0.4 V less than the actual battery voltage because of the diode drop on the battery board to prevent damage due to incorrect installation of the batteries. From 8/27/09 to 9/8/09, the parameters stored in FLASH on each Imote2 were uploaded many times to optimize
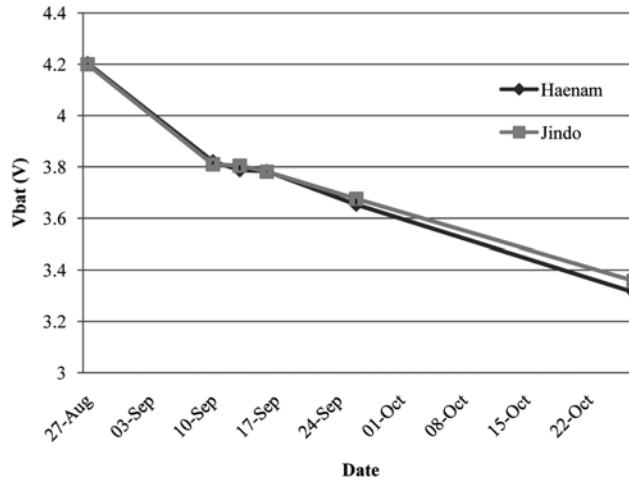
Fig. 21 Average on-board voltage

network performance, which is a power demanding procedure. After 9/8/09, the *AutoMonitor* application has run continuously to measure the data. During this period, the power consumption has been approximately linear. The minimum onboard voltage for sensing is 3.4 V. The power consumption depends on the frequency of data measurement, data length, and sleeping parameters. Based on once-a-day measurement with the network parameters mentioned in Table 2, three D-cell batteries can operate about two months.

6.5 Energy harvesting strategy using solar power

In total, eight sensor nodes employ solar panels and rechargeable batteries. Five of the solar powered sensor nodes are on the cables, two on the pylons, and one on the deck. Fig. 22 shows the voltage of the solar rechargeable batteries during monitoring. The voltage levels of the rechargeable
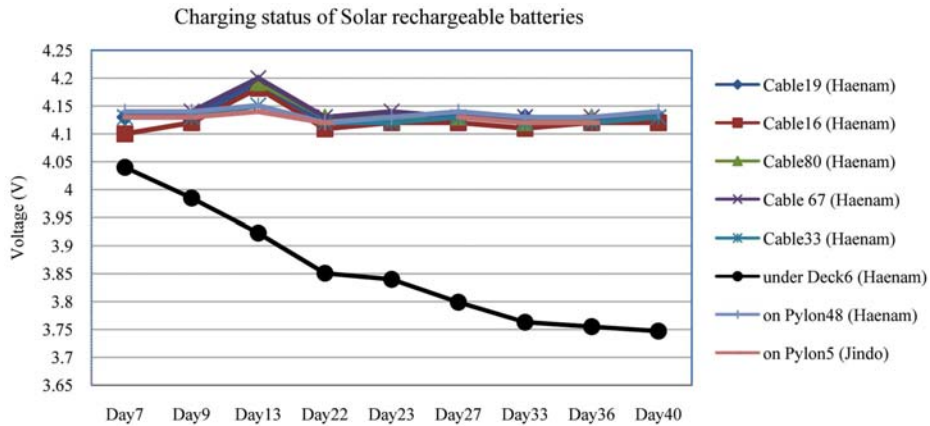

Fig. 22 Charging status of solar rechargeable batteries on Jindo Bridge SHM system

battery have maintained around 4.15 V, which confirms that the charging process of the solar power system is working well. However, the solar powered node located under the deck (Haenam side, node 6) shows a continuous decrease in the voltage level. The reason for the decrease is that it only can receive indirect reflected sunlight, because its orientation is downward. Either a more sensitive solar panel, reorienting the panel, or another type of energy harvesting system should be considered for sensors located under the deck in the next deployment.

7. Conclusions

A state-of-the-art SHM system using a WSSN has been successfully deployed on the Jindo Bridge in South Korea to verify the performance of the system and to serve as a driver for advancement of smart sensor technology. The Imote2 has been selected as the wireless sensor platform to use along with custom-designed SHM-A and SHM-W sensor boards. An autonomous structural monitoring system has been developed employing a threshold detection strategy and an energy-efficient sleeping mode to extend the network lifetime. Solar powered nodes have been employed to investigate the possibility of energy harvesting to power the sensor network.

In total, 70 sensor nodes have been installed, divided into two sub-networks to decrease the communication time and because of the limit of the radio communication range. All sensors are carefully located based on radio communication capability determined by extensive radio communication tests. The measured data shows a good agreement with data from the existing wired system, which verifies that the data quality of the WSSN is reliable. Successful deployment of this WSSN demonstrates the suitability of the Imote2 smart sensor platform, the SHM-A sensor board, and the ISHMP software for full-scale, continuous, autonomous SHM.

Acknowledgements

References

Abe, M., Fujino, Y., Yanagihara, M. and Sato, M. (2000), "Monitoring of hakucho suspension bridge by ambient vibration measurement", *Proceedings of the Nondestructive Evaluation of Highways, Utilities, and Pipelines IV,* Newport Beach, USA, March.

Antenova (2009), *Titanis: p/n B4844/B6090*, http://www.antenova.com/?id=536.

Çelebi, M., Purvis, R., Hartnagel, B., Gupta, S., Clogston, P., Yen, P., O'Connor, J. and Franke, M. (2004), "Seismic instrumentation of the Bill Emerson Memorial Mississippi River Bridge at Cape Girardeau (MO): A cooperative effort", *Proceedings of the 4th International Seismic Highway Conference*, Memphis, Tenn, USA.

Crossbow Technology (2009), *Imote2-High-performance Wireless Sensor Network Node*, http://www.xbow.com/Products/Product_pdf_files/Wireless_pdf/Imote2_Datasheet.pdf.

Crossbow Technology (2007), *Imote2 Hardware Reference Manual, Revision A,* http://www.xbow.com/Support/Support_pdf_files/Imote2_Hardware_Reference_Manual.pdf.

Cho, S., Jo, H., Jang, S., Park, J., Jung, H.J., Yun, C.B., Spencer, Jr., B.F. and Seo, J. (2010), "Structural health monitoring of a cable-stayed bridge using smart sensor technology: data analysis", *Smart Struct. Syst.*, **6**(5-6), 461-480.

Doebling, S.W., Farrar, C.R. and Cornwell, P. (1997), "A statistical comparison of impact and ambient testing results from the alamosa canyon bridge", *Proceedings of the 15th International Modal Analysis Conference*.

FHWA (2009), *Deficient Bridges by State and Highway System*, http://www.fhwa.dot.gov/bridge/nbi/defbr09.cfm

Jang, S., Rice, J.A., Li, J., Jo, H., Spencer, Jr., B.F. and Wang, Z. (2009), "Structural monitoring of a historic truss bridge using a wireless sensor network", *Proceedings of the Asia-Pacific Workshop on Structural Health Monitoring*.

Kim, S., Pakzad, S., Culler, D.E., Demmel, D., Fenves, G., Glaser, S. and Turon, M. (2007), "Health monitoring of civil infrastructures using wireless sensor networks", *Proceedings of the 6th International Conference on Information Processing in Sensor Networks*.

Linderman, L.E., Rice, J.A., Barot, S., Spencer, Jr., B.F. and Bernhard, J.T. (2010), *Characterization of Wireless Smart Sensor Performance*, Newmark Civil Engineering Laboratory Report 21, http://hdl.handle.net/2142/15101.

Lynch, J.P., Wang, Y., Loh, K.J., Yi, J.H. and Yun, C.B. (2006), "Performance monitoring of the geumdang bridge using a dense network of high-resolution wireless sensors", *Smart Mater. Struct.*, **15**, 1561-1575.

Mechitov, K., Kim, W., Agha, G. and Nagayama, T. (2004), "High-frequency distributed sensing for structure monitoring", *Proceedings of the First International Workshop on Networked Sensing Systems*, Tokyo, Japan.

MEMSIC Inc. (2010), *ITS400, Imote2 Basic Sensor Board*, http://www.xbow.com/Products/Product_pdf_files/Wireless_pdf/ITS400_Datasheet.pdf.

Miller, T. and Spencer, Jr., B.F. (2009), *Solar energy harvesting and software enhancements for autonomous wireless smart sensor networks,* NSEL Report Series, University of Illinois at Urbana-Champaign.

Nagayama, T. and Spencer, Jr., B.F. (2007), *Structural Health Monitoring using Smart Sensors*, Newmark Structural Engineering Laboratory Report Series 001, http://hdl.handle.net/2142/3521.

Pakzad, S. (2008), *Statistical Approach to Structural Monitoring Using Scalable Wireless Sensor Networks*, Ph.D. Dissertation, University of California, Berkeley.

Powerizer (2009), *Polymer Li-Ion Module: 3.7 V 10000mAh (37Wh, 5.0A rate) - Prewired with PCB (PL9059156), UN Approved (3.0)*, http://www.batteryspace.com/polymerli-ionmodule37v10000mah37wh85arate-prewiredwithpcbpl9059156.aspx.

Rice, J.A., Mechitov, K.A., Spencer, Jr., B.F. and Agha, G. (2008), "A service-oriented architecture for structural health monitoring using smart sensors", *Proceedings of the 14th World Conference on Earthquake Engineering*, Beijing, China.

Rice, J.A. and Spencer, Jr., B.F. (2009), *Flexible Smart Sensor Framework for Autonomous Full-scale Structural Health Monitoring*, Newmark Structural Engineering Laboratory Report Series 018, http://hdl.handle.net/2142/13635.

Rice, J.A., Mechitov, K., Sim, S.H., Nagayama, T., Jang, S., Kim, R., Spencer, Jr., B.F., Agha, G. and Fujino, Y. (2010), "Flexible smart sensor framework for autonomous structural health monitoring", *Smart Struct. Syst.,* **6**(5-6), 423-438.

Roundy, S., Wright, P.K. and Rabaey, J.M. (2004), *Energy Scavenging for Wireless Sensor Networks,* Kluwer Academic Publishers.

Sim, S.H. and Spencer, Jr., B.F. (2009), *Decentralized Strategies for Monitoring Structures using Smart Sensor Networks,* Newmark Structural Engineering Laboratory Report Series 019, http://hdl.handle.net/2142/14280.

Spencer, Jr., B.F. and Nagayama, T. (2006), "Smart sensor technology: a new paradigm for structural health monitoring", *Proceedings of the Asia-Pacific Workshop on Structural Health Monitoring, keynote lecture*, Yokohama, Japan.

Todd, M., Johnson, G., Vohra, S., Chen-Chang, C., Danver, B. and Malsawma, L. (1999), "Civil infrastructure monitoring with fiber Bragg grating sensor arrays", *Proceedings of the 2nd International Workshop on Structural Health Monitoring*.

Wong, K.Y. (2004), "Instrumentation and health monitoring of cable-supported bridges", *Struct. Control Health Monit.*, **11**(2), 91-124.